

PHz current switching in calcium fluoride single crystal

Ojoon Kwon and D. Kim

Citation: [Applied Physics Letters](#) **108**, 191112 (2016); doi: 10.1063/1.4949487

View online: <http://dx.doi.org/10.1063/1.4949487>

View Table of Contents: <http://scitation.aip.org/content/aip/journal/apl/108/19?ver=pdfcov>

Published by the [AIP Publishing](#)

Articles you may be interested in

[Nonlinear luminescence response of CaF₂:Eu and YAIO₃:Ce to single-ion excitation](#)

J. Appl. Phys. **115**, 033108 (2014); 10.1063/1.4861152

[Scintillation characteristics of LiCaAlF₆-based single crystals under X-ray excitation](#)

Appl. Phys. Lett. **102**, 161907 (2013); 10.1063/1.4803047

[Crystal field disorder effects in the optical spectra of Nd³⁺ and Yb³⁺-doped calcium lithium niobium gallium garnets laser crystals and ceramics](#)

J. Appl. Phys. **112**, 063110 (2012); 10.1063/1.4752070

[Photoelectric effects of ultraviolet fast response and high sensitivity in LiNbO₃ single crystal](#)

J. Appl. Phys. **106**, 023114 (2009); 10.1063/1.3183957

[Crystallographic effects in micro/nanomachining of single-crystal calcium fluoride](#)

J. Vac. Sci. Technol. B **22**, 46 (2004); 10.1116/1.1633770

A promotional banner for Applied Physics Reviews. On the left is a thumbnail of a review article cover titled 'AIP Applied Physics Reviews' with a diagram of a layered structure. The main text reads 'NEW Special Topic Sections' in large white letters. Below this, it says 'NOW ONLINE' in yellow, followed by 'Lithium Niobate Properties and Applications: Reviews of Emerging Trends' in white. The AIP Applied Physics Reviews logo is in the bottom right corner.

NEW Special Topic Sections

NOW ONLINE
Lithium Niobate Properties and Applications:
Reviews of Emerging Trends

AIP Applied Physics
Reviews

PHz current switching in calcium fluoride single crystal

Ojoon Kwon^{1,2} and D. Kim^{1,2,a)}

¹Department of Physics, Center for Attosecond Science and Technology, Pohang University of Science and Technology, Pohang 37673, South Korea

²Max Planck Center for Attosecond Science, Max Planck POSTECH/Korea Res. Init., Pohang 37673, South Korea

(Received 20 February 2016; accepted 2 May 2016; published online 12 May 2016)

We demonstrate that a current can be induced and switched in a sub-femtosecond time-scale in an insulating calcium fluoride single crystal by an intense optical field. This measurement indicates that a sizable current can be generated and also controlled by an optical field in a dielectric medium, implying the capability of rapid current switching at a rate of optical frequency, PHz (10^{15} Hz), which is a couple of orders of magnitude higher than that of contemporary electronic signal processing. This demonstration may serve to facilitate the development of ultrafast devices in PHz frequency. *Published by AIP Publishing.* [<http://dx.doi.org/10.1063/1.4949487>]

The computing industry, which is based on integrated electronic circuits, has been advancing at such a rapid pace that it has now become feasible to perform a vast volume of information processing in a short time at a low cost.¹ The continually increasing volume of information to be processed demands that processing, even in a smaller-sized circuitry, be completed at a faster clock rate. In the past, the density of transistors in integrated circuits has increased exponentially,² doubling every two years (Moore's Law). Recently, however, the growth rate of this development has decelerated due to physical and fundamental obstacles,³ e.g., the appearance of false bits due to thermal fluctuation,⁴ known as Johnson–Nyquist noise.^{5,6} Hence, for faster processing, it is currently even more critical to increase the clock rate. Contemporary electrical interconnections, however, possess intrinsic limitations because the interconnecting wires need to be charged. The charging of wires inevitably requires time and induces heat generation. Moreover, the more densely integrated electronic chips become and the higher their clock rate, the more severe the heat generation problem. Considering the limitations established by energy cost, it is clear that neither improvement of integration density nor clock rate constitutes an ultimate solution.⁷ While progress in electric interconnections is hindered by the aforementioned factors, the feasibility of optical means has arisen as a viable alternative.^{8,9} Light is a prospective way for carrying information, free from both heat dissipation and charging time. While there have been efforts to develop optical functional components,^{10,11} e.g., modulators,¹² waveguides,¹³ receivers,^{14,15} transistors,¹⁶ and memory,¹⁷ attention has also been paid to combining optics with electronics.^{18–20} For example, the electrical current induced by a light field has been reported in fused silica by Schiffrin *et al.*²¹ and also in sapphire and calcium fluoride by Kwon *et al.*,²² suggesting the viability of optical control of a current in an optical medium. These observations can be explained by the creation of Wannier–Stark states from valence and conduction band when the medium is subjected to light field. Under the influence of sufficiently strong optical field, the promotion for valence band electrons to conduction band becomes considerably

probable, giving rise to transient conductivity, namely, semi-metalization. Here, by studying the light-induced current in calcium fluoride, we address the following question: how fast can the current be switched from one direction to the opposite in CaF₂? We selected calcium fluoride as our specimen in order to claim that this method is not restricted to a certain material but extensively applicable to various species of medium. It possesses a large band gap (12 eV)²³ in comparison with the photon energy (~ 1.5 eV) so that it should not undergo single photon processes but highly nonlinear processes. Besides, CaF₂ has distinct properties from SiO₂, especially in crystallographic viewpoint. For instance, while SiO₂ exhibits non-centrosymmetry, piezoelectric effect, and birefringence, CaF₂ does not show any of them.

Figure 1 shows the experimental layout. Carrier-envelope-phase (CEP)-stabilized few-cycle pulses of ~ 4 fs FWHM (full width at half maximum) are used. They are separated into two arms to form an interferometer. Each arm of the interferometer is equipped with a motorized wedge pair, enabling the independent control of CEP. The periscopes are placed in such a way that the polarization of one arm is perpendicular to that of the other arm. Optical pulses from two arms are focused and spatially overlapped onto a calcium fluoride substrate, on which two metal electrodes are facing each other with a spacing of $10\ \mu\text{m}$. A pulse in one arm is temporally delayed with respect to that in the other arm with an adjustable optical path length. The current between the two electrodes is converted into voltage and amplified by a gain of 10^8 V/A in a current amplifier. We introduce a modulation to CEP at half a repetition rate, and use a lock-in amplifier referenced at the CEP modulation frequency. Consequently, CEP-independent components are extinct, and only CEP-dependent contribution is extracted by the lock-in amplifier. Utilizing this setup, we performed two kinds of experiments: single pulse and two pulse.

First, using a single pulse from either of the arms in the apparatus (Figure 2(a)), the transferred charge per pulse Q with respect to the insertion of a wedge is measured at a given field strength of $2.6\ \text{V}/\text{\AA}$ for parallel and perpendicular polarization. The translation of the wedge alters the thickness of medium which laser pulses travel. Since the propagation of

^{a)}kimd@postech.ac.kr

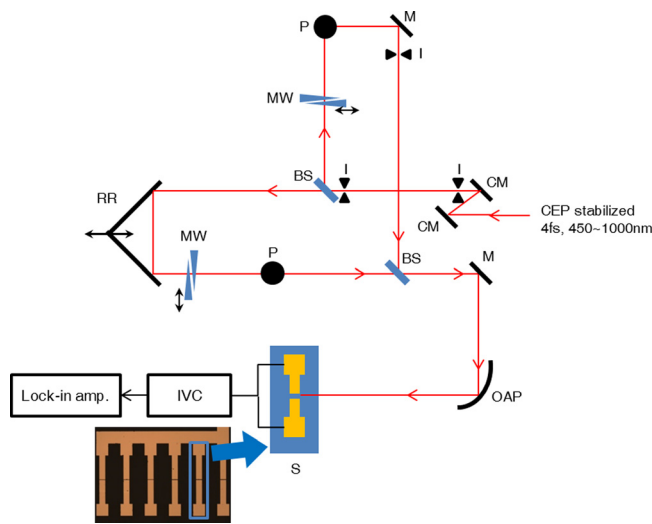


FIG. 1. Schematic drawing of the experimental layout. CEP-stabilized few-cycle laser pulses are split into two arms, composing an interferometer. The CEP of the laser pulse train is controlled, such that the waveform of a laser pulse is the opposite sign of that of the adjacent pulse. In other words, the CEP is modulated at half of the repetition rate. The polarization of one arm is rotated by 90° using a periscope. Two orthogonally-polarized pulses with an alterable time delay are focused onto a sample by an off-axis parabola. Owing to motorized wedges, the CEP of each arm is controlled independently. The current collected by two electrodes facing each other is amplified and converted into a voltage signal in the current-to-voltage converter. Then, the voltage output of the current amplifier is fed to a lock-in amplifier referenced at a rate of CEP modulation. Due to the lock-in amplifier, only the CEP-dependent current is picked up. Inset on the lower left corner depicts the microscope image of real specimen electrodes patterned on CaF_2 substrate via photo lithography method. Blue rectangle on the microscope image corresponds to the sample in the main figure, denoted by symbol “S.” Symbols in the figure represent the following. CM: chirped mirror; I: iris diaphragm; BS: beamsplitter; MW: motorized wedge pair; P: periscope; M: mirror; RR: retro reflector with adjustable time delay; OAP: off-axis parabolic mirror; S: sample; and IVC: current-to-voltage converter, or current amplifier.

laser pulses in refractive media shifts CEP proportional to propagation length,²⁴ the displacement of the wedge is equivalent to the change of CEP $\Delta\phi$ (horizontal axis of Figure 2(b)). Around and above a field strength of $\sim 2.7 \text{ V/\AA}$, CaF_2 may

undergo dielectric breakdown. If the medium experiences dielectric breakdown, the magnitude of transferred charge diminishes permanently. Whenever such an aspect is noticed, the data are discarded so that all the data presented in this work are ensured to be free from laser-induced damage. First, a large difference in amplitude is observed. When the channel between electrodes is laid parallel to the polarization (blue), the transferred charge is decreased by a factor of 15 compared with the case when the channel is placed perpendicular to the polarization (red). Two orthogonally polarized pulses play distinctive roles: (1) the pulses polarized parallel to the groove between electrodes on the substrate populates charge carriers in the substrate, but the charge carriers are not yet collected by the electrodes since they are driven by the optical field parallel to the electrodes. The geometrical projected area of current on the electrodes is so small that few charges are captured by electrodes and detected as a current. Hereafter, this pulse is termed the “injection field” because it promotes electrons from a valence band to a conduction band, i.e., injecting charge carriers to the medium. (2) The pulses polarized perpendicular to the groove direct injected charge carriers toward the electrodes. The significant portion is collected, and the imbalance of charges collected by the two electrodes is detected as an electric current. This pulse is referred to as the “driving field” hereafter since it influences the flow of charge carriers. The reason for a still small, but nonzero, current in the case of the parallel polarization may be that real situations deviated from the ideal case: (1) a small, but nonzero, polarization component which directs charges toward the electrodes; (2) it is still possible that there exists a slight misalignment of polarization with respect to the groove, both of which still drive the current to the electrodes; and (3) microscopic geometrical imperfection of electrodes. Another important aspect noticed is an oscillatory feature. In Figure 2(b), the current exhibits an oscillation whose period corresponds to that of the modulation of CEP introduced by a wedge displacement. Considering the symmetry of the driving optical field, the asymmetry of the current collected by the electrodes is maximized at A and A', when the optical waveform is cosine-like,

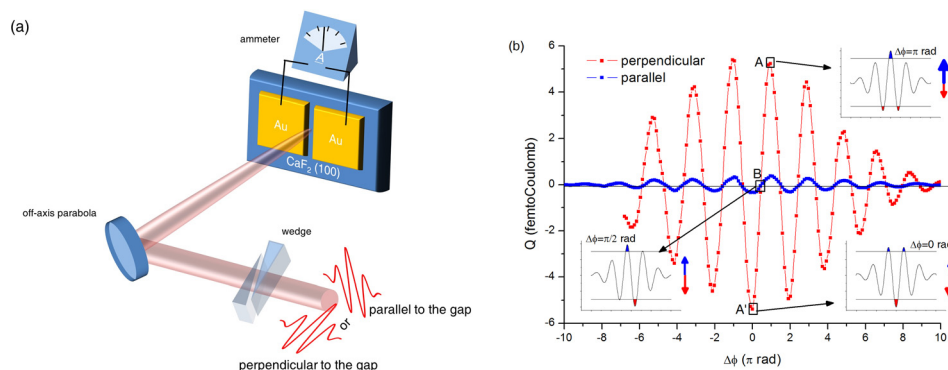


FIG. 2. (a) Schematic illustration of the experimental setup used with a single arm of the interferometer. The polarization of an incident pulse can be either parallel or perpendicular to the electrode junction. The CEP is varied by a pair of wedges. (b) Transferred charge per pulse Q as a function of $\Delta\phi$ at a field strength of 2.6 V/\AA for parallel (blue) and perpendicular (red) polarization to the channel. Insets in corners describe the direction of the current induced by each cycle of the optical field and the sign of the net current (blue and red arrows) within the entire duration of the pulse at a given CEP (marked by A, A', and B). Horizontal lines in insets denote the critical field, above which charge carrier population becomes significant. As shown in the two insets on the right-hand side, when the waveform is an even function, i.e., symmetric with respect to the vertical axis, the charge transfer toward one direction is dominant (as indicated by the length and thickness of arrows). On the other hand, the inset in the lower-left corner shows that, in the case of odd symmetry waveform, the current toward each electrode over the pulse duration is equal. Consequently, currents flowing in opposite directions are cancelled out, resulting in a negligible net current.

as illustrated in the insets in the upper-right (we set this phase to be $\phi = \pi$ rad) and the lower-right ($\phi = 0$ rad) corners in Figure 2(b), respectively. On the contrary, when the waveform is sine-like (ϕ is a half of an odd integer multiplied by π radian), the inset in the lower-left corner of Figure 2(b), an equal amount of charges are collected by the two electrodes facing each other, resulting in zero net current (B). The dependence on polarization and periodicity in accordance with optical field oscillation implies that the current is induced by the instantaneous field of optical pulse. It is also found that Q decreases as $|\Delta\phi|$ increases. This is because of the temporal broadening of optical pulses due to an additional dispersion by wedges, which effectively decreases the field strength. Since Q increases near-exponentially against field strength, as discussed in Ref. 22, the insertion of wedges for CEP control leads to the reduction of Q .

Second, we performed a series of measurements using two pulses from both arms of the interferometer (Figure 3(a)), in which one pulse (parallel polarization to the electrode joint) plays the role of injection field, and the other (perpendicular polarization) driving field independently. The injection field is expected to create charge carriers without inducing any current. In contrast, the driving field is so weak that it does not populate charge carriers by itself, but rather directs the charge carriers to the electrodes. The injection field is set to have a peak field strength of 2.3 V/\AA , and the driving field has a peak field strength of 0.3 V/\AA . The phase ϕ_i of the injection field is set to $\phi_i = +\frac{\pi}{2}$ rad, so that there is no residual current (B in Figure 2(b)). The phase ϕ_d of the driving field is set to either $\phi_d = +\frac{\pi}{2}$ rad (blue) or $\phi_d = -\frac{\pi}{2}$ rad (red). Q is measured as a function of time delay Δt between the injection and the driving fields at given field strengths and phases. The noise level of the raw data ($\sim 0.1 \text{ fC}$) is rather high in comparison with nontrivial signal level ($\sim 0.2 \text{ fC}$). For the sake of clearer discernibility, the curves are processed using the fast Fourier transform (FFT) method, applying a high pass filter of cutoff frequency at 0.35 PHz (Figure 3(b)).

As it is reported in Ref. 22, a charge increases near-exponentially with respect to an instantaneous field strength. Especially, the increase of charge becomes prominent at the critical field.²⁵ Consequently, for a field higher than the

critical field, the probability of the promotion for valence band electrons to conduction band increases drastically, implying substantial charge carrier injection. In the two-pulse scheme, therefore, the injection of charge carriers mostly occurs at the moment the peak field strength of the injection field reaches or exceeds the critical field strength, which is temporally concentrated within a fraction of its optical cycle and thus implicitly limited to a time span much shorter than the driving field period. Since injected charges are directed by the instantaneous driving field, the temporal modulation of the driving field is translated to charge transfer as a function of time delay, exhibiting agreement in the period of $\sim 2.5 \text{ fs}$. The sign of the current is inverted as the CEP of the driving field is shifted by π radian. All of the above observations strongly support that the oscillation of Q as a function of Δt is construed as the transcript of the oscillation of the driving field. We assert that the current is created and driven in the dielectric medium by the instantaneous field of laser pulses.

Although noise level is subdued by means of the aforementioned FFT filtering process, the region of meaningful periodicity and sign inversion is still limited to ± 1 optical cycle in the vicinity of $\Delta t = 0$. For delays greater than 2.5 fs , these aspects disappear. This is due to the fact that at such a delay of greater than 2.5 fs , the effective temporal overlap of the injection and the driving field becomes weak. The magnitude of the first cycle of driving field after $\Delta t = 0$ diminishes drastically as the driving field is delayed with respect to the injection field by more than 2.5 fs . This is also the case when the driving field precedes the injection field by more than 2.5 fs . As the instantaneous driving field strength gets weaker, it is less likely to observe phase-dependent feature.

Note that, near $\Delta t = 0$ in Figure 3(b), the current emerges from zero to a peak value within a quarter of an optical period, or 0.7 fs . This observation demonstrates that the current can be switched in a sub-femtosecond time-scale and controlled at an optical frequency. Hence, the insulator-to-semimetal transition occurs in a sub-femtosecond time-scale. We can estimate the transient conductivity of calcium fluoride by considering the amount of the current at temporal overlap, the driving field strength at the moment, and the effective cross section. The effective cross section is described in Ref. 22. The transferred

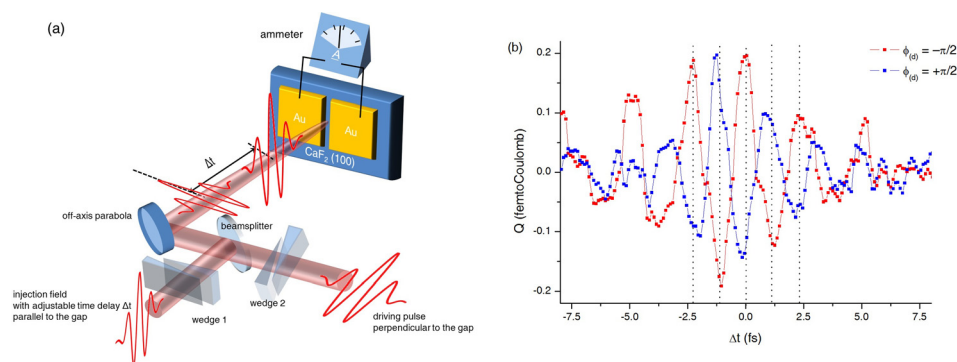


FIG. 3. (a) Schematic illustration of the two-pulse measurement. The injection field (polarized parallel to the electrode junction) collinearly propagates with the driving field (polarized perpendicular to the junction) with a variable time delay. Independent control of the CEP of pulses in each arm is implemented by wedge pairs. (b) Transferred charge per pulse Q versus time delay Δt between the injection and driving field. For a negative delay, the driving pulse precedes the injection pulse. The peak field strength of injection field is 2.3 V/\AA and that of driving field is 0.3 V/\AA . The CEPs of the injection field is fixed to $\phi_i = +\pi/2$. Measurements are conducted under two opposite waveforms (or CEP shifted by π radian) of the driving field, i.e., $\phi_d = +\pi/2$ (blue) and $\phi_d = -\pi/2$ (red). The curves are processed by FFT high pass filtering with a cutoff frequency at 0.35 PHz . Dotted vertical lines are guidelines to eyes to indicate sign inversion during the temporal overlap of the injection and driving field.

charge per pulse, Q , can be written as $Q = A_{\text{eff}} \int_{-\infty}^{\infty} j(t) dt$, where A_{eff} is the effective cross section and $j(t)$ the current density.²¹ The maximum $Q(\Delta t = 0)$ is about 0.2 fC at $E_0^{(d)} \approx 0.3 \text{ V/\AA}$, $A_{\text{eff}} \approx 2.53 \times 10^{-11} \text{ m}^2$, and the duration of the current density pulse is on the order of 1 fs. The peak current density is, thus, about $J \approx 7.9 \times 10^9 \text{ A/m}^2$. The electrical conductivity is estimated to be $\sigma = J/E_0^{(d)} \approx 2.7(\Omega \cdot \text{m})^{-1}$. Though the static conductivity of calcium fluoride has not yet been reported, considering the conductivity of typical insulators, one can estimate that it may be on the order of $\sim 10^{-16} (\Omega \cdot \text{m})^{-1}$. Our observation indicates that the conductivity of calcium fluoride is markedly increased, i.e., by 16 orders of magnitude within a one-femtosecond time-scale by an optical field.

In summary, we demonstrate that a sizable current can be switched in calcium fluoride within 1 fs. The conductivity of calcium fluoride is enhanced by a factor of 10^{16} under the influence of an intense optical transient. We believe that this work may serve as the basis for the development of devices for ultrafast current control at a time-scale of a femtosecond or PHz rate.

The authors thank Professor F. Krausz of Max Planck Institute for Quantum Optics and his group members for sharing the measurement technology and providing valuable guidance. This research has been supported in part by Global Research Laboratory Program [Grant No. 2009-00439] and by Max Planck POSTECH/KOREA Research Initiative Program [Grant No. 2011-0031558] through the National Research Foundation of Korea (NRF) funded by Ministry of Science, ICT & Future Planning.

¹D. A. B. Miller, *Appl. Opt.* **49**(25), F59 (2010).

²G. E. Moore, *Proc. IEEE* **86**(1), 82 (1998).

³H. J. Caulfield and S. Dolev, *Nat. Photonics* **4**(5), 261 (2010).

⁴L. B. Kish, *Phys. Lett. A* **305**(3), 144 (2002).

⁵J. B. Johnson, *Phys. Rev.* **32**(1), 97 (1928).

⁶H. Nyquist, *Phys. Rev.* **32**(1), 110 (1928).

⁷F. Krausz and M. I. Stockman, *Nat. Photonics* **8**(3), 205 (2014).

⁸D. A. B. Miller, *Proc. IEEE* **97**(7), 1166 (2009).

⁹M. Stucchi, S. Cosemans, J. Van Campenhout, Z. Tókei, and G. Beyer, *Microelectron. Eng.* **112**, 84 (2013).

¹⁰B. Aleksandr and B. Keren, *Rep. Prog. Phys.* **75**(4), 046402 (2012).

¹¹M. Haurylau, G. Chen, H. Chen, J. Zhang, N. Nelson, D. H. Albonese, E. G. Friedman, and P. M. Fauchet, *IEEE J. Sel. Top. Quantum Electron.* **12**(6), 1699 (2006).

¹²K. Preston, Po. Dong, B. Schmidt, and M. Lipson, *Appl. Phys. Lett.* **92**(15), 151104 (2008).

¹³B. G. Lee, C. Xiaogang, A. Biberman, L. Xiaoping, I. W. Hsieh, C. Cheng-Yun, J. I. Dadap, X. Fengnian, W. M. J. Green, L. Sekaric, Y. A. Vlasov, R. M. Osgood, and K. Bergman, *IEEE Photonics Technol. Lett.* **20**(6), 398 (2008).

¹⁴M. W. Geis, S. J. Spector, M. E. Grein, J. U. Yoon, D. M. Lennon, and T. M. Lyszczarz, *Opt. Express* **17**(7), 5193 (2009).

¹⁵K. Preston, Y. Ho, D. Lee, M. Zhang, and M. Lipson, *Opt. Lett.* **36**(1), 52 (2011).

¹⁶W. Chen, K. M. Beck, R. Bücken, M. Gullans, M. D. Lukin, H. Tanji-Suzuki, and V. Vuletić, *Science* **341**(6147), 768 (2013).

¹⁷E. Kuramochi and M. Notomi, *Nat. Photonics* **9**(11), 712 (2015).

¹⁸S. Mishra, N. K. Chaudhary, and K. Singh, *International J. of Scientific and Engineering Research* **3**(4), 390–396 (2012).

¹⁹N. Kirman, M. Kirman, R. K. Dokania, J. F. Martinez, A. B. Apsel, M. A. Watkins, and D. H. Albonese, paper presented at the Proceedings of the 39th Annual IEEE/ACM International Symposium on Microarchitecture (2006).

²⁰G. Chen, H. Chen, M. Haurylau, N. A. Nelson, D. H. Albonese, P. M. Fauchet, and E. G. Friedman, *VLSI J.* **40**(4), 434 (2007).

²¹A. Schiffrin, T. Paasch-Colberg, N. Karpowicz, V. Apalkov, D. Gerster, S. Muhlbrandt, M. Korbman, J. Reichert, M. Schultze, S. Holzner, J. V. Barth, R. Kienberger, R. Ernstorfer, V. S. Yakovlev, M. I. Stockman, and F. Krausz, *Nature* **493**(7430), 70 (2013).

²²O. Kwon, T. Paasch-Colberg, V. Apalkov, B.-K. Kim, Ju.-J. Kim, M. I. Stockman, and D. Kim, *Sci. Rep.* **6**, 21272 (2016).

²³G. W. Rubloff, *Phys. Rev. B* **5**(2), 662 (1972).

²⁴L. Xu, T. W. Hänsch, Ch. Spielmann, A. Poppe, T. Brabec, and F. Krausz, *Opt. Lett.* **21**(24), 2008 (1996).

²⁵S. Ghimire, N. Georges, D. DiChiara Anthony, S. Emily, I. Stockman Mark, A. Pierre, F. DiMauro Louis, and A. R. David, *J. Phys. B* **47**(20), 204030 (2014).